Received: 20 February 2023 | Revised: 18 August 2023 | Accepted: 30 August 2023

DOI: 10.1002/hbm.26485

RESEARCH ARTICLE

WILEY

Compressed primary-to-transmodal gradient is accompanied with subcortical alterations and linked to neurotransmitters and cellular signatures in major depressive disorder

Yang Xiao [1,2,3] | Lei Zhao [1,2,3] | Xuelian Zang [1,2,3] | Shao-Wei Xue [1,2,3]

[1]Center for Cognition and Brain Disorders, The Affiliated Hospital of Hangzhou Normal University, Hangzhou, Zhejiang Province, PR China

[2]Institute of Psychological Science, Hangzhou Normal University, Hangzhou, Zhejiang Province, PR China

[3]Zhejiang Key Laboratory for Research in Assessment of Cognitive Impairments, Hangzhou, Zhejiang Province, PR China

Correspondence
Shao-Wei Xue, Center for Cognition and Brain Disorders, Hangzhou Normal University, No. 2318, Yuhangtang Road, Hangzhou 311121, Zhejiang, China.
Email: xuedrm@126.com

Funding information
Natural Science Foundation of Zhejiang Province, Grant/Award Number: LY17H180007; Key Medical Disciplines of Hangzhou, Zhejiang Medical and Health Science and Technology Project, Grant/Award Number: 2022490271; Affiliated Hospital of Hangzhou Normal University, Grant/Award Numbers: 2021YN2021105, KY21085

Abstract

Major depressive disorder (MDD) has been shown to involve widespread changes in low-level sensorimotor and higher-level cognitive functions. Recent research found that a primary-to-transmodal gradient could capture a cortical hierarchical organization ranging from perception and action to cognition in healthy subjects, but a prominent gradient dysfunction in MDD patients. However, whether and how this cortical gradient is linked to subcortical impairments and whether it is reflected in the microscale neurotransmitter systems and cell type-specific transcriptional signatures remain largely unknown. Data were acquired from 323 MDD patients and 328 sex- and age-matched healthy controls derived from the REST-meta-MDD project, and the human brain neurotransmitter systems density maps and gene expression data were drawn from two publicly available datasets. We investigated alterations of the primary-to-transmodal gradient in MDD patients and their correlations with clinical symptoms of depression and anxiety, as well as their paralleled subcortical impairments. The correlations between MDD-related gradient alterations and densities of the neurotransmitter systems and gene expression information were assessed, respectively. The results demonstrated that MDD patients had a compressed primary-to-transmodal gradient accompanied by paralleled alterations in subcortical regions including the caudate, amygdala, and thalamus. The case–control gradient differences were spatially correlated with the densities of the neurotransmitter systems including the serotonin and dopamine receptors, and meanwhile with gene expression enriched in astrocytes, excitatory and inhibitory neuronal cells. These findings mapped the paralleled subcortical impairments in cortical hierarchical organization and also helped us understand the possible molecular and cellular substrates of the co-occurrence of high-level cognitive impairments with low-level sensorimotor abnormalities in MDD.

KEYWORDS
astrocytes, cellular signature, functional connectivity, functional connectome gradient, major depressive disorder, neurotransmitter

1 | INTRODUCTION

Major depressive disorder (MDD) is a common and highly heterogeneous psychiatric condition characterized by pervasive and persistent low mood, accompanied by diminished interests, cognitive dysfunction, and physical symptoms (Drysdale et al., 2017). Previous studies on the brain mechanisms underlying MDD mainly focused on emotional dysregulation and high-level cognitive deficits (Zhao et al., 2021), while an increasing number of studies attached significance to MDD-related low-level sensorimotor processes, such as visual processing (Bubl et al., 2010) and pain perception (Fitzgerald, 2013). However, the abnormal co-occurrence or transition of high-level cognitive processing with low-level sensorimotor activity underlying MDD clinical characteristics is still poorly understood, and possible microscale neurobiological signatures and macroscale neuroimaging indexes in the brain are especially needed to explain these abnormalities.

As a fundamental organizational principle for information processing, brain network hierarchy was thought to direct the propagation of low-level sensorimotor information along multiple cortical relays into high-level transmodal areas, which responsible for processing increasingly abstract and complex information (Huntenburg et al., 2018). By combining resting-state functional magnetic resonance imaging techniques and a manifold learning method, researchers recently mapped brain network hierarchy in a gradient manner (Margulies et al., 2016). This gradient method complemented discrete anatomical and functional parcellation approaches and incorporated potentially signal-mixed brain connectomes into continuous representations along the cortical surface (Huntenburg et al., 2017). Typically, the principal primary-to-transmodal gradient could be described as an intrinsic geometry of the cortex which started with primary sensory and motor regions, and extended to the hierarchical apex of brain systems, including the default mode network (DMN) and some transmodal regions (Haueis, 2021). The gradient could separate specific information processing (such as sensory and cognitive processes) from high-level processes and achieve gradually transitioning from low-level processes to high-level functional attributes in healthy participants (Haak & Beckmann, 2020; Hong et al., 2019; Sepulcre et al., 2012). Given the concurrence of sensation and cognitive processing abnormality in patients with MDD, the description of the primary-to-transmodal gradient in MDD probably enabled us to understand this co-deficit from the brain hierarchy organizational principal perspective. Along this pattern, it might be hypothesized that MDD patients might present successive destruction between low-level and high-level brain networks. In addition to the increasingly recognized cortical functional impairments in patients with MDD, accumulating studies emphasized that the paralleled alterations in subcortical regions (Chung et al., 2011; Mayberg, 1997; Phelps & LeDoux, 2005). Indeed, prior studies showed that the dysregulated interactions of subcortical and cortical systems might involve the MDD-related pathological mechanism, including deficits in the amygdala-prefrontal (Anderson Collins, Chin, et al., 2020), frontal-striatal (Greene et al., 2020), and thalamus-prefrontal circuits (Siegel et al., 2014). These impaired subcortical and cortical alterations offered additional insights into illuminating brain multiple system-wide integration and the neurobiological underpinnings of MDD. However, how the subcortical areas exhibit paralleling disruptions with cortical gradient remains poorly understood.

MDD-related changes in the macroscale brain organizational hierarchy might be regulated or reflected by some microscale factors such as neurotransmitters, gene expression, and cells. Positron emission tomography (PET) and single photon computed tomography (SPECT) imaging provided the whole-brain density distribution of some neurotransmitter systems such as dopamine, serotonin, and neuropeptides (Dukart et al., 2021; Hesse et al., 2017; Kaller et al., 2017). Using a neuroimaging-neurotransmitter association analysis method, previous studies found that abnormal brain functional activity was closely associated with dopaminergic and serotonergic dysfunction in depression and schizophrenia (Chen et al., 2021; Malhotra et al., 1998; Park et al., 2022). Recent studies on schizophrenia have also confirmed the imbalanced relationship between neurotransmitters and brain functional networks (Conio et al., 2020). On the other hand, the microarray dataset of Allen Human Brain Atlas (AHBA) could establish a connection between the microscale transcriptome gene profiles and macroscale brain networks (Elman et al., 2017; Fornito et al., 2019; Hibar et al., 2015). A previous connectome–transcriptome association study showed that the structural connectome in MDD patients was associated with gene expression profiles which ontologically enriched synapse-related terms (Li, Seidlitz, et al., 2021). The gene enrichment techniques and emerging single-cell expression data also enabled us to assess the relationship between cell type-specific gene expressions and neuroimaging phenotypes (Seidlitz et al., 2020). For instance, previous studies pointed out that cortical somatostatin interneurons and astrocytes might be related to the abnormal neuroimaging phenotypes of MDD (Anderson, Collins, Kong, et al., 2020). Recent study found that the primary-to-transmodal gradient of MDD patients was associated with gene expression involving transsynaptic signaling and calcium ion binding (Xia et al., 2022). However, there is limited knowledge regarding whether and how neurotransmitter systems and cell type-specific transcriptional signatures reflect the impaired primary-to-transmodal gradient in MDD.

In the present study, we were to examine the MDD-related primary-to-transmodel gradient with its paralleled subcortical alterations, and characterize the neurotransmitter systems and cell type-specific transcriptional signatures which accounted for the abnormal functional connectome gradient. Using a dataset drawn from the multicenter data meta-analysis project for resting-state functional magnetic resonance imaging (fMRI) of depression (REST-meta-MDD), we first revealed the abnormal gradient patterns and their related subcortical impairments in MDD patients. We then investigated their genetic associations and neurotransmitter substrates based on publicly available data (Dukart et al., 2021; Hibar et al., 2015). This exploratory research highlighted subcortical alterations associated with MDD-related cortical hierarchical organization and helped us understand the possible molecular and cellular substrates of the co-occurrence of high-level emotional and cognitive deficits with low-level sensorimotor abnormalities in MDD.

2 | MATERIALS AND METHODS

2.1 | Phenotypic and imaging dataset

The demographic and clinical characteristics of the participants were summarized in Table 1. Three hundred and twenty-three MDD patients and 328 healthy controls (HC) were included in the present study. The participants were part of the DIRECT Consortium (Chen et al., 2022; Yan et al., 2019) for publicly available data of brain imaging of depression (http://rfmri.org/REST-meta-MDD). More information about the inclusion and exclusion criteria can be seen in our Supporting Information. The contributing sample size and data acquisition parameters of each site can be found in Table S1, and demographic data and group differences by site can be found in Table S2. The diagnosis of MDD was determined by the criteria of the Diagnostic and Statistical Manual of Mental Disorders, Fourth Edition (DSM-IV) or the International Classification of Diseases 10 (ICD-10) criteria for MDD. The depression severity was assessed by the 17-item Hamilton Rating Scale for depression (HAMD) and anxiety severity was rated using the Hamilton Anxiety Scale (HAMA). The site differences in HAMD and HAMA scores were found in Table S3. The study has been approved by the ethics committees of each site and written informed consent was received from each subject prior to the formal testing. Brain image preprocessing was performed according to a standardized protocol using the DPARSF software (http://www.rfmri.org/) and details were described in the Supporting Information.

2.2 | Functional connectome gradient analysis

The functional connectome gradient was mapped by using the BrainSpace toolbox (http://github.com/MICA-MNI/BrainSpace). For each participant, functional connectivity (FC) matrices were first computed using Pearson's correlation coefficient based on the average time series of all region of interest pairs from 980 parcels using Zalesky's template and then normalized using Fisher's *z*-transformation (Zalesky et al., 2010). Following previous research (Margulies et al., 2016), a cosine similarity matrix was constructed to capture connectivity topographical similarities based on the top 10% of FC and further scaled to a normalized angle matrix. The diffusion map embedding was implemented to decompose the normalized angle matrix into the gradient components, which explained connectivity variations across different brain areas. Following previous studies, we set the α parameter of the present gradient algorithm to 0.5 in the diffusion process (Haak & Beckmann, 2020; Margulies et al., 2016; Park et al., 2022). After constructing group-level gradient template which were generated from a mean FC matrix across all MDD and HC participants, the gradient components of each participant were finally realigned in the group-level gradient template by applying the Procrustes rotation approaches, ensuring that subsequent analyses were conducted on the same gradient architecture across all participants (Figure 1a).

The gradient measurements were calculated at global level and regional level. Three global level measurements for the first two connectome gradients were calculated, including the gradient variation, gradient dispersion, and gradient range. Specifically, the gradient variation was calculated as the variance of the given gradient values, indicating the standard deviation of the gradient scores across the whole brain, and a greater variation reflected a higher heterogeneity in the connectivity pattern across brain regions. The gradient dispersion was measured as the squared Euclidean distance between the centroid of each pair of subnetworks in the gradient space determined by the first two gradients. A greater dispersion value meant a more discrete distribution between different subnetworks in the gradient space. The gradient range was defined as the difference between the highest positive and lowest negative values of the given gradient values. A larger gradient range indicated a greater differentiation in the encoded connectivity pattern between the regions located at the opposite ends of the gradient. For the regional level gradient, the gradient score of each region served as the gradient measurement of this region and gradient measurements of each subnetwork were achieved by the abovementioned Yeo' s functional network partition (Yeo et al., 2011). We utilized the ComBat model to correct the site

TABLE 1 Demographic data and group differences.

Characteristics	MDD (mean ± SD)	HC (mean ± SD)	t/χ^2	*p*
Sex (M/F)	323 (120/203)	328 (113/215)	0.516	.472[a]
Age (years)	35.149 ± 11.767	34.872 ± 14.265	0.270	.788[b]
Mean FD	0.105 ± 0.038	0.109 ± 0.040	−1.263	.207[b]
Education level (years)	11.195 ± 3.280	13.150 ± 3.507	−8.304	<.001[b]
HAMD scores	20.889 ± 5.648			
HAMA scores	20.845 ± 8.091			
Duration of illness (months)[c]	46.874 ± 60.726			
On medication/non-medication/unknown	112/109/102			

Abbreviations: F, female; FD, framewise-displacement; HAMA, Hamilton Anxiety Scale; HAMD, 17-item Hamilton Rating Scale for depression; HC, healthy control; M, male; MDD, major depressive disorder; SD, standard deviation.

[a]The *p*-value was obtained by a chi-square test.

[b]The *p*-value was obtained by a two-tailed two-sample *t*-test.

[c]Data on the duration of illness was available for 277 patients.

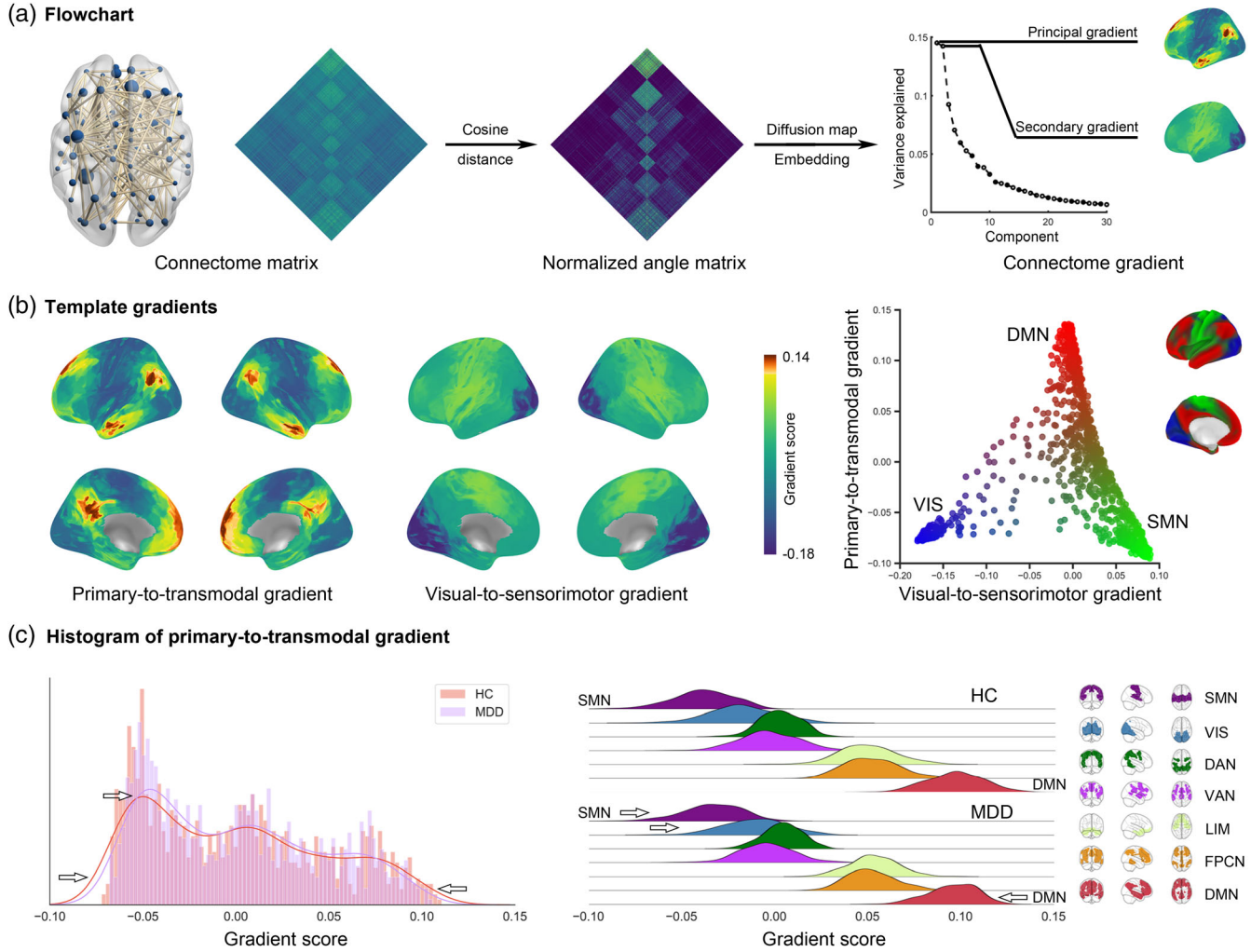

FIGURE 1 The flowchart for mapping functional connectome gradients. (a) The cortical functional connectivity matrix (left) was transformed to a normalized angle matrix (middle) and the diffusion map embedding was used to capture the gradient components. (b) The core connectome gradients in the MDD patients and controls, including the principal gradient (left) and the second core gradient (middle). The scatter plot of the first two gradients represented the gradient space (right). (c) Global (left) and system-based (right) histograms showing extreme values were suppressed in MDD compared to controls while those in the mid-range increased, indicating a compressed primary-to-transmodal gradient in MDD. Arrows indicated the direction of the significant differences between the MDD ad controls. DAN, dorsal attention network; DMN, default mode network; FPCN, frontoparietal control network; HC, healthy controls; LIM, limbic network; MDD, major depressive disorder; SMN, sensorimotor network; VAN, ventral attention network; VIS, visual network.

effects on the gradient maps and measurements with age, sex, and diagnosis as covariates (Xia et al., 2022; Yu et al., 2018). Besides, we also investigated the associations between primary-to-transmodel gradient and brain network topology indexes in MDD (Supporting Information).

The case–control gradient differences were computed by using independent-sample *t*-test with age, sex, years of education, and head motion (mean framewise-displacement [FD]) as covariates. The threshold of statistical significance was set at 0.05 and correction for multiple comparisons was performed using the false discovery rate (FDR corrected). The Pearson correlation analysis was performed to investigate the associations between all abnormal gradient measurements and clinical features with age, sex, education level, and mean FD as covariates. The significance level threshold was set at $p < .05$ with FDR correction. The mediation analysis was conducted to assess whether global gradient metrics were mediators in the relationship between the HAMA scores and HAMD scores, or vice versa. The mediation analysis was conducted using the mediation package in R. The detailed steps to be examined were: (1) effect *c* (the total effect) indicated the relationship between HAMA scores and HAMD scores; (2) effect *a* meant the relationship between HAMA scores and gradient metrics (i.e., gradient range); (3) effect *b* represented the relationship between gradient metrics and HAMD scores; and (4) effect *ab* (the indirect effect) meant the indirect effect between HAMA and HAMD scores, indicating whether the relationship between HAMA and HAMD scores was significantly reduced after controlling for gradient metrics. The effect *c*′ indicated a direct effect after controlling the mediation effect. Participants' age, sex, educational level, and head motion (mean FD) were controlled as covariates in all mediation analyses. The significance of the indirect effects was tested based on

10,000 nonparametric bootstrapping with a 95% confidence interval (CI) that did not include zero.

2.3 | Subcortical-weighted gradients

We used the subcortical-weighted gradient to examine MDD-related subcortical parallel impairments accompanied with the alteration in cortical gradient (Park, Bethlehem, et al., 2021; Park, Hong, et al., 2021). Specifically, the subcortical structures of each brain hemisphere were first parcellated into the accumbens, amygdala, caudate, hippocampus, pallidum, putamen, and thalamus according to the Harvard–Oxford subcortical structural atlas (Kennedy et al., 1998). Subcortical–cortical FC maps (14 × 980) were constructed by computing the Pearson correlation coefficients between the average time series of the subcortical and cortical regions. For group analyses, the correlation coefficients were converted using Fisher's *z*-transformation to improve normality. The subcortical-weighted gradient was generated by weighting cortical gradient space (determined by the first two gradients) with the subcortical–cortical FC matrix and projected into subcortical regions. The case–control differences of the subcortical-weighted gradient were assessed using independent-sample *t*-test after controlling for age, sex, education level, and head motion (mean FD).

2.4 | Associations between connectome gradient dysfunction in MDD and neurotransmitter systems

We tried to characterize the molecular architecture of neurotransmitter systems underlying the MDD-related gradient alterations by evaluating the spatial relationship between the gradient alterations and density distribution of neurotransmitter systems derived from prior PET/SPECT studies (Dukart et al., 2021; Park et al., 2022). Following prior studies (Chen et al., 2021; Park et al., 2022), we adopt 10 neurotransmitter systems including receptors of 5-HT1a, 5-HT1b, 5-HT2a, D1, and D2, transporters of dopamine transporter, noradrenaline transporter (NAT), serotonin transporter, and neurotransmitters of 18F fluorodopa and gamma-aminobutyric acid a (GABAa; https://github.com/juryxy/JuSpace). We first linearly rescaled all PET/SPECT maps to make neurotransmitter intensity values between 0 and 100 and then averaged densities across 980 regions defined by Zalesky's template. We calculated the spatial correlations between the case–control *t*-map values and each neurotransmitter map. The significance of the correlation coefficients was assessed using 10,000 times spherical rotations-based spatial autocorrelation, corrected permutation test followed by FDR to adjust for multiple comparisons.

2.5 | Gene expression dataset and preprocessing

The gene expression data was obtained from six neurotypical adult donors in the AHBA (http://human.brain-map.org). This gene microarray data of brain tissue samples was preprocessed using the abagen toolbox (https://www.github.com/netneurolab/abagen) according to a recommended pipeline (Arnatkeviciute et al., 2019). Briefly, the genetic probes were reannotated using the information provided by previously published guidelines. The intensity-based filtering was performed to filter those probes with values that did not exceed the background noise and the threshold was set as 50%. Each of all tissue sample was spatially registered to the Montreal Neurological Institute (MNI) coordinate space according to the T1-weighted images of each donor, and tissue samples were assigned to brain regions based on their MNI coordinates (https://github.com/chrisfilo/alleninf). Following a previous well-done study about connectome gradient, the microarray data was mapped onto a cortical parcellation with 360 brain regions defined by Glasser's atlas (Xia et al., 2022). Considering right hemisphere data was available from only two donors, gene expression analysis was conducted in 180 regions of the left hemisphere. Some brain regions that could not be assigned to any tissue sample were excluded following previous studies, resulting in the remaining 148 brain regions. Gene expression values were normalized for each donor across brain regions using a robust sigmoid function and then rescaled to the unit interval. Finally, a gene expression map (148 regions × 15,631 genes) was obtained for further gradient-transcriptome association analysis.

2.6 | Identification of MDD-related genes associated with the altered primary-to-transmodal gradient in MDD

To capture the genetic correlation with the MDD-related changes of the primary-to-transmodal gradient, we performed the gradient-transcriptome association analysis using partial least squares regression (PLS). Specifically, we aligned the case–control differences of the primary-to-transmodal gradient to the Glasser's atlas respectively. The PLS was adopted to identify the association between the expression patterns for all 15,631 genes and the case–control differences in the primary-to-transmodal gradient. The gene expression data and the case–control gradient differences were set as the predictor variable and the response variable, respectively. The statistical significance of the variance explained by the PLS components was tested based on spherical rotations using a spatial autocorrelation corrected permutation analysis (10,000 times). For the significant PLS component map, we computed the spatial correlations between the weighted gene expressions and case–control gradient differences. The significance of the correlation coefficient was tested using a permutation analysis (10,000 times). Finally, the PLS weight of each gene was transformed into a *z*-score value by dividing the weight by the standard deviation. The standard deviation of the corresponding weights is derived from 10,000 instances of bootstrapping. We ranked all genes according to their *z*-score weights in the PLS components. We tested the null hypothesis of zero weight for each gene based on univariate one-sample *Z* tests, and the list of genes with an FDR of 1‰ (positively or negatively) was called as the PLS gene list

corresponding to MDD-related regional alterations in the primary-to-transmodal gradient.

We wanted to further capture the relationships between MDD-related changes of the primary-to-transmodal gradient and MDD-related genes. All 24 MDD-related genes were first identified based on previous well-done research (Li, Seidlitz, et al., 2021), including *ADRA2A*, *AVPR1B*, *CHRM2*, *CNR1*, *CREB1*, *CRH*, *CRHR1*, *CRHR2*, *CUX2*, *GAD2*, *GPR50*, *HTR1A*, *HTR1B*, *HTR1D*, *HTR3A*, *HTR5A*, *MAOA*, *PDE1A*, *SLC6A2*, *SLC6A4*, *SST*, *TAC1*, *TPH1*, and *TPH2*. We screened the 12 genes that overlapped with the 15,631 background genes in the AHBA dataset and accessed their relationships with the gradient alteration. Significance was set at $p < .05$ with 10,000 times spatial autocorrelation corrected permutation test and adjusted by FDR.

2.7 | MDD-related cell type-specific gene expression

We exploratory analyzed differential gene expression for each cell type in a brain sample from microarray data, and seven specific cell classes were adopted including astrocytes, excitatory neurons, inhibitory neurons, microglia, endothelial cells, oligodendrocyte precursors and oligodendrocytes. The gene sets of each cell type were obtained from previous large-scale single-cell studies using postmortem cortical samples (Di Biase et al., 2022; Li, Seidlitz, et al., 2021; Seidlitz et al., 2020). We overlapped the gene set of each cell type with the PLS1 rank gene list, and then computed the number of overlapped genes in each cell type. The significant level of the number of the overlapped genes was set at $p < .05$ with 10,000 times spatial autocorrelation corrected permutation test and adjusted by FDR. The overlapped genes of each cell type were included in the gene enrichment analysis for interpreting the biological insights of gene expression data using Metascape analysis (https://metascape.org/gp/index.html#/main/step1). The statistically significant level of enrichment analysis was set to $p < .05$ with FDR correction.

3 | RESULTS

3.1 | Connectome gradient dysfunction in MDD

The gradient analysis flowchart was shown in Figure 1. In the present study, we focused on the first two principal components capturing the maximum connectome variance (Figure 1b). The first or primary-to-transmodal gradient was anchored at one end by the primary network (which included the visual network [VIS] and sensorimotor network [SMN]), and at the other by the transmodal or DMN regions. The second or visual-to-sensorimotor gradient was organized along a gradual axis defined by the VIS at one end and the SMN at the other. The gradient space was established with a coordinate system in which the *y*-axis indicated the primary-to-transmodal gradient and the *x*-axis measured the visual-to-sensorimotor gradient. In the coordinate system, the gradient variables of the DMN regions were plotted in the upper extreme while those of the primary networks were found in the lower extreme (Figure 1b). As shown in Figure 1c, the histogram of the primary-to-transmodal gradient exhibited a compressed hierarchical organization in MDD compared to HC, indicating a trend toward a dedifferentiated connectome profile between the primary network and DMN. The subnetwork-level gradient scores were acquired according to Yeo's functional network template. The system-based histogram showed that MDD patients had increased gradient values in the VIS and SMN, but decreased values in the DMN.

As shown in Figure 2a, there were statistically significant case–control differences using three global measures including the gradient variation ($t = -4.216$, $p < .001$, Cohen's $d = -0.331$), dispersion ($t = -2.443$, $p = .015$, Cohen's $d = -0.192$), and range ($t = -4.836$, $p < .001$, Cohen's $d = -0.379$). The MDD group exhibited significant correlations between the HAMD scores and three measures including the gradient variation ($r = -0.176$, $p = .002$), gradient dispersion ($r = -0.139$, $p = .013$), and gradient range ($r = -0.188$, $p < .001$). Additionally, the gradient range was significantly correlated with the HAMA scores in MDD ($r = -0.120$, $p = .032$). Results from the mediation effect analysis showed that the gradient range partially mediated the relationship between the HAMA and HAMD scores ($ab = 0.016$, $p = .026$, 95% CI = [0.0012, 0.0395]). There were no significant mediation effects of coping on the relationship between the HAMD and HAMA scores when the gradient range was as the mediated variable.

The case–control comparison results of the regional level gradient were shown in Figure 2b. Compared with HC, MDD patients showed significantly lower gradient scores in the DMN ($t = -4.074$, $p < .001$, FDR corrected, Cohen's $d = -0.315$), but higher scores in the VIS ($t = 3.269$, $p = .003$, FDR corrected, Cohen's $d = 0.296$) and SMN ($t = 3.335$, $p = .003$, FDR corrected, Cohen's $d = 0.261$). The gradient scores of the VIS, SMN, and DMN were significantly correlated with the HAMD scores in MDD (VIS: $r = 0.135$, $p = .026$; SMN: $r = 0.140$, $p = .026$; DMN: $r = -0.175$, $p = .012$; FDR corrected). No significant case–control differences between the global or regional level gradient measures were observed in the sensorimotor-to-visual gradient.

3.2 | Subcortical-weighted gradients

As shown in Figure 3, the case–control comparison results showed that the subcortical-weighted gradients in the left and right caudate ($t = -3.151$, $p = .024$, FDR corrected, Cohen's $d = -0.247$ and $t = -2.783$, $p = .039$, FDR corrected, Cohen's $d = -0.218$) were significantly decreased in MDD. Additionally, MDD exhibited a decrease in the left thalamus ($t = -2.232$, $p = .026$, uncorrected) and an increase in the right amygdala ($t = 2.394$, $p = .017$, uncorrected).

3.3 | Associations between connectome gradient dysfunction in MDD and neurotransmitter systems

Figure 4a showed a flowchart for building spatial correlations of a cortex-wide neurotransmitter map with the case–control connectome

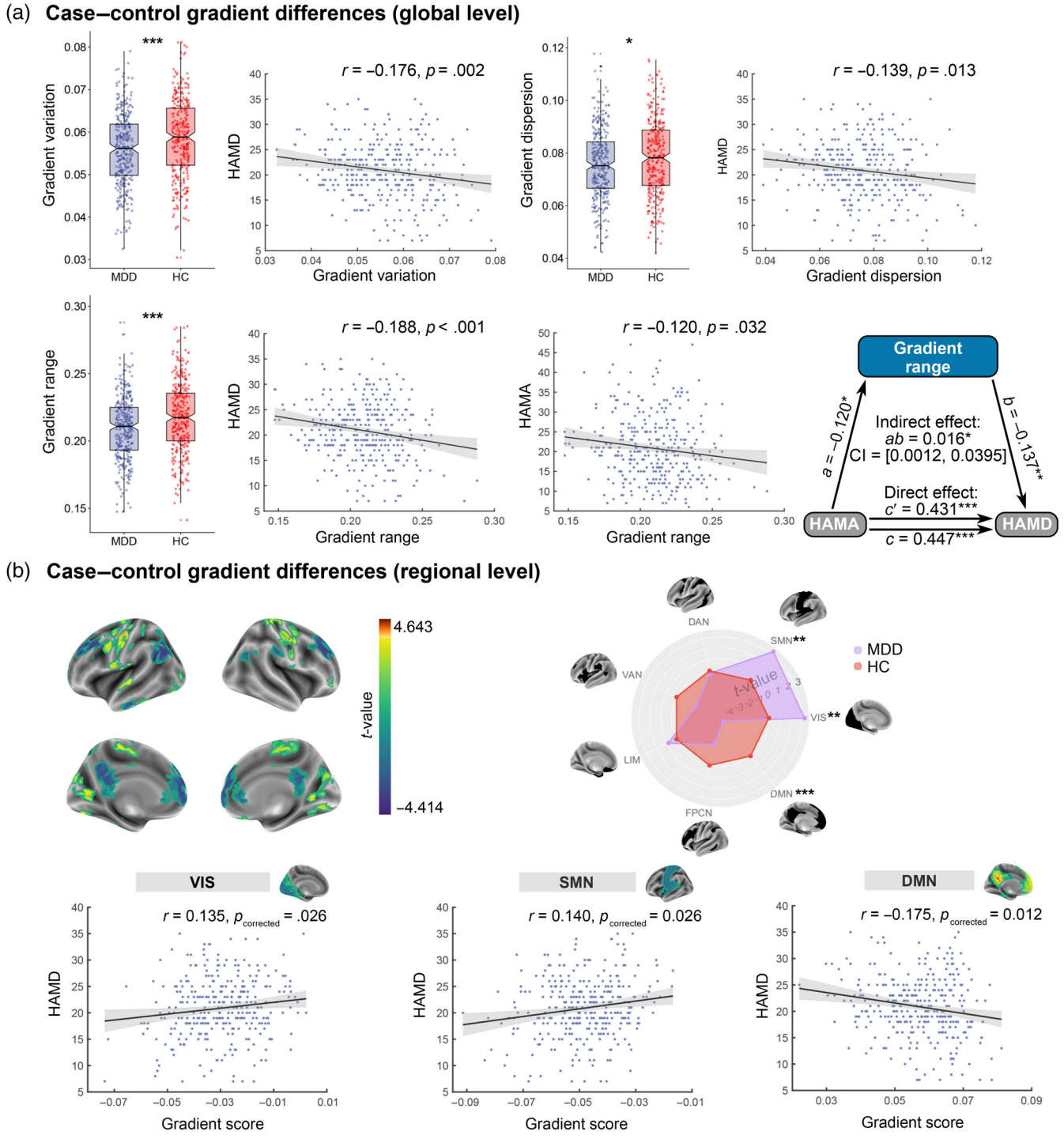

FIGURE 2 Case–control gradient differences of the primary-to-transmodal gradient in MDD. (a) Global level case–control gradient differences of the primary-to-transmodal gradient. All three global measures exhibited significant case–control differences and significant correlations with the HAMD scores. The gradient range was significantly correlated with the HAMA scores, and partially mediated the relationship between the HAMA scores and the HAMD scores. (b) Regional level case–control gradient differences of the primary-to-transmodal gradient. Surface-wide statistical comparisons between MDD and HC indicated significant increases/decreases in MDD in red/blue. The spider plots (right) indicated a significantly decreased DMN gradient score in MDD and an increase in the VIS and SMN compared with the controls. Scatter diagram of the correlations between the abnormal gradient scores of three functional networks and the HAMD scores in MDD. ***$p < .001$; **$p < .01$; *$p < .05$. CI, confidence intervals; DAN, dorsal attention network; DMN, default mode network; FDR, false discovery rate; FPCN, frontoparietal control network; HAMA, Hamilton Anxiety Scale; HAMD, Hamilton Rating Scale for depression; HC, healthy controls; LIM, limbic network; MDD, major depressive disorder; SMN, sensorimotor network; VAN, ventral attention network; VIS, visual network.

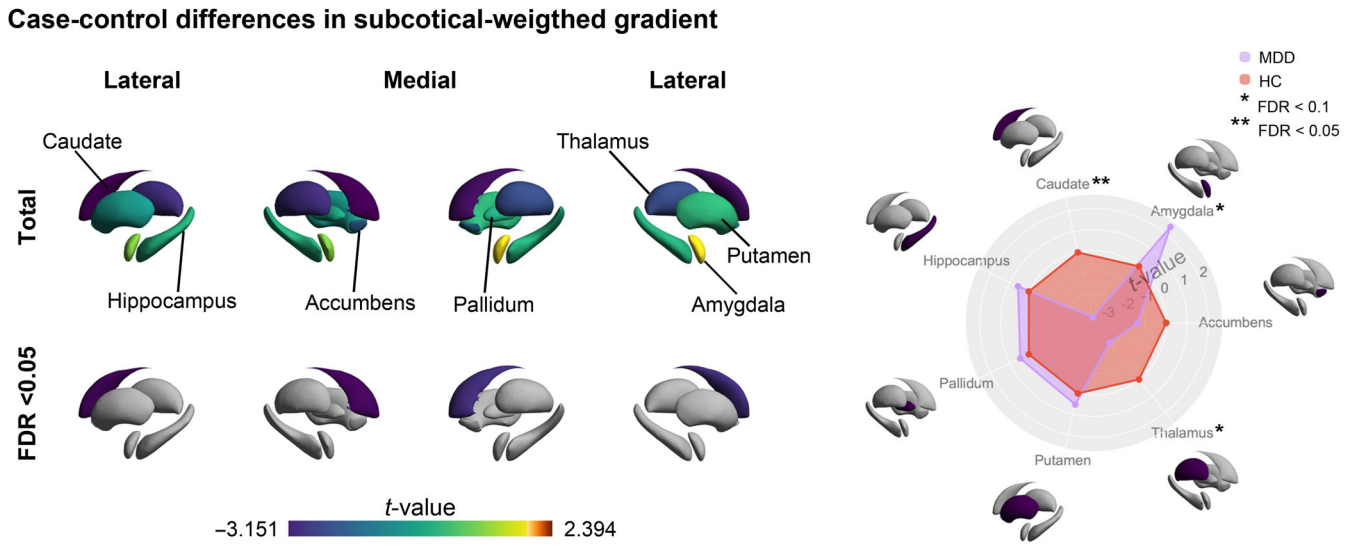

FIGURE 3 The case–control differences in the subcortical-weighted gradient. $^{**}p < .05$, FDR corrected; $^{*}p < .05$, uncorrected. MDD, major depressive disorder; HC, healthy controls; FDR, false discovery rate.

gradient differences. As shown in Figure 4b, the case–control differences of the primary-to-transmodal gradient demonstrated statistically significant negative associations with 5-HT1a, 5-HT1b, 5-HT2a, and D1 receptor densities (5-HT1a: $r = -0.23$, $p < .001$; 5-HT1b: $r = -0.083$, $p = .015$; 5-HT2a: $r = -0.137$, $p < .001$; D1: $r = -0.131$, $p < .001$), and positive correlations with NAT density ($r = 0.085$, $p = .015$). The significance was based on 10,000 times permutation tests with spatial autocorrelation correction and adjusted by FDR.

3.4 | Cell type-specific gene expression of the MDD-related alterations in the primary-to-transmodal gradient

The cortical gene expression profiles corresponding to the case–control gradient differences were shown in Figure 5. The brain surface on the left side of Figure 6a mapped the case–control differences of the primary-to-transmodal gradient. The right subplot of Figure 5a indicated the spatial gene expression organization in the brain, which presented high expression mainly in the parietal–occipital areas and low expression in the prefrontal areas based on the first PLS component (PLS1). The scatterplot in the middle side of Figure 5a indicated that the PLS1 values were significantly positively related to the case–control gradient differences in the primary-to-transmodal gradient ($r = 0.521$, $p < .001$). There were 1079 positively weighted (PLS1+) and 1129 negatively weighted (PLS1−) genes at a threshold value of FDR of 1‰. As shown in Figure 5b, there were 12 MDD-related genes that overlapped with the 15,631 AHBA background genes. Therein, six gene expressions exhibited statistically significant correlations with the case–control t values, including five negative correlations (*CNR1*: $r = -0.294$, $p = .009$; *HTR1A*: $r = -0.231$, $p = .022$; *MAOA*: $r = -0.217$, $p = .022$; *PDE1A*: $r = -0.237$, $p = .022$; and *SST*: $r = -0.263$, $p = .022$) and a positive correlation (*CUX2*: $r = 0.303$, $p = .009$). The *CNR1* and *CUX2* gene expression exhibited the largest negative correlation and positive correlation with case–control gradient differences in MDD, respectively. The significance was based on 10,000 times permutation tests with spatial autocorrelation correction and adjusted by FDR.

The spatial distribution of the genes that overlapped between seven cell type-specific genes and the fore-mentioned PLS1− gene list was described in Figure 6a. As shown in Figure 6b, the gene list was significantly involved in astrocytes, excitatory and inhibitory neurons (astrocytes: number = 181, $p < .001$; excitatory neurons: number = 95, $p < .001$; inhibitory neurons: number = 84, $p = .033$; 10,000 times permutation tests with spatial autocorrelation and adjusted by FDR). The Gene Ontology enrichment analysis of cell type-specific genes indicated that the case–control gradient differences were significantly enriched ($p < .05$, FDR corrected) for biological processes associated with astrocytes and neurons, mainly including signaling, biological regulation, and cellular process (Figure 6c).

4 | DISCUSSION

The present study characterized MDD-related cortical functional alterations from a perspective of functional connectome gradient and further searched for other possible macroscale neuroimaging indexes and microscale neurobiological signatures to explain these changes. Specifically, we identified that subcortical paralleled impairments were mainly in the caudate, amygdala, and thalamus. We found that the neurotransmitter systems which were associated with the abnormal primary-to-transmodal gradient in MDD mainly involved the serotonin and dopamine. Besides, our integrative analysis of imaging and transcriptomic data established an association between MDD-related gradient changes and gene expression enriched in astrocytes, excitatory and inhibitory neurons. This research found abnormal cortical hierarchical organization was accompanied with subcortical impairments

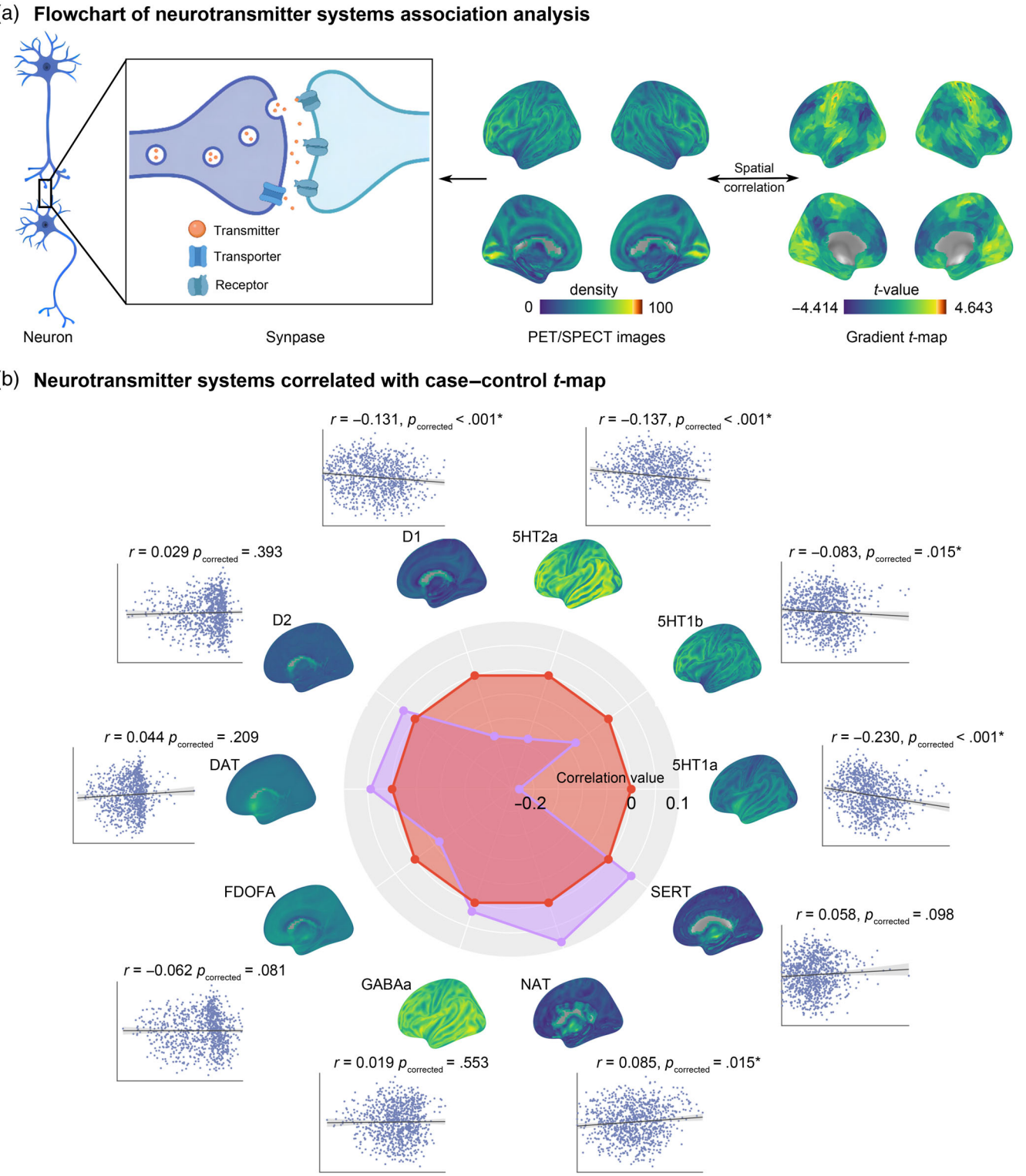

FIGURE 4 The associations between MDD-related gradient alteration and distributions of neurotransmitter systems. (a) Flowchart of neurotransmitter system association analysis. (b) Spatial correlations of each neurotransmitter map with case–control gradient difference *t*-map. The radar plot showed the correlation coefficients value. *$p < .05$, 10,000 times permutation tests with spatial autocorrelation and adjusted by false discovery rate (FDR). DAT, dopamine transporter; FDOPA, 18F fluorodopa; GABAa, gamma-aminobutyric acid a; NAT, noradrenaline transporter; SERT, serotonin transporter.

and linked to molecular architectures and cell type-specific transcriptional signatures in MDD, which could yield new insights toward an integrative understanding of MDD pathophysiology.

We found that the primary-to-transmodal gradient in MDD exhibited a prominent compression with regional tunings in the primary network and DMN. Specifically, the smaller gradient spatial

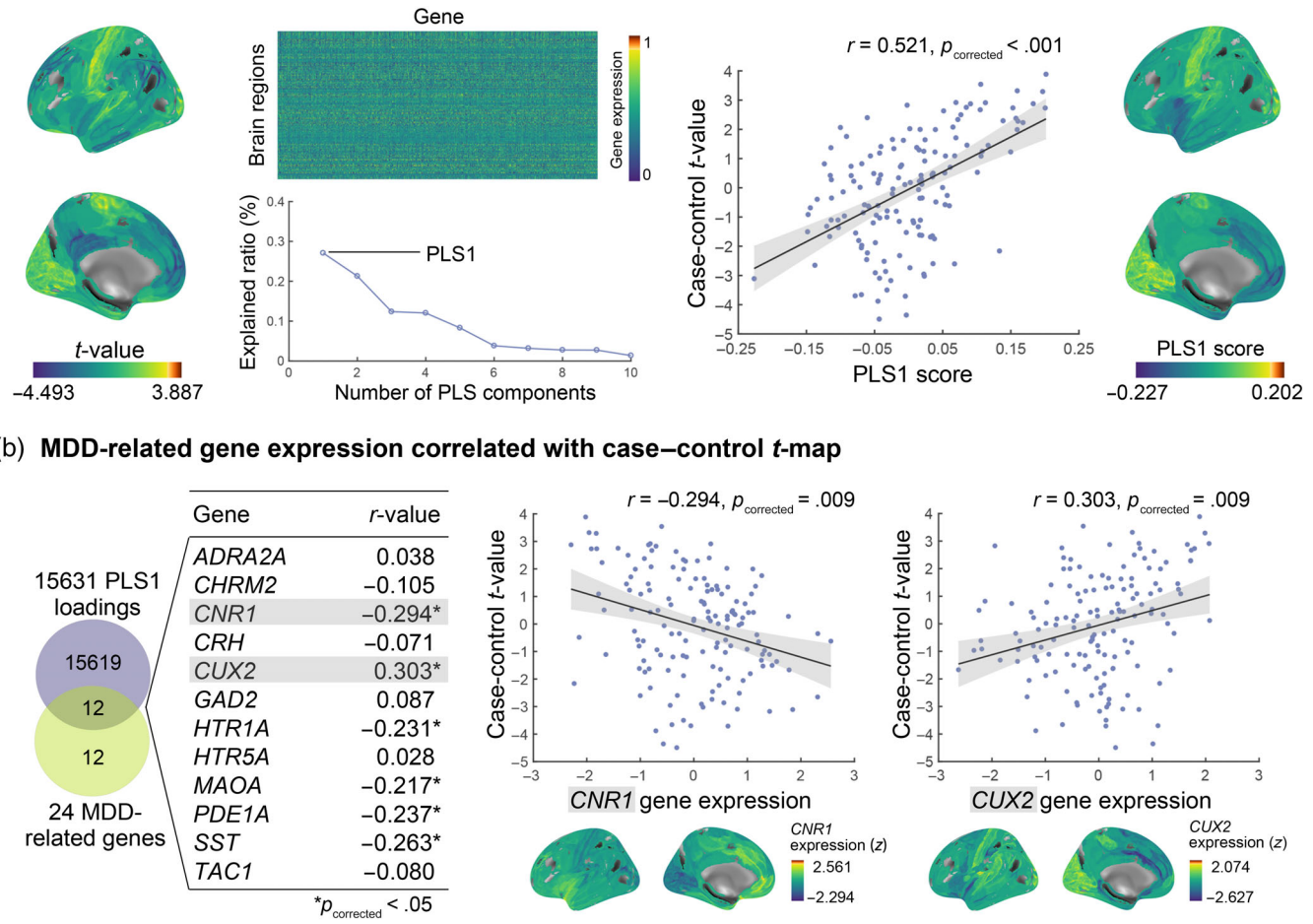

FIGURE 5 Gene expression profiles related to the primary-to-transmodal gradient alterations in MDD. (a) The case–control *t*-values of the primary-to-transmodal gradient were mapped onto the brain surface (left). The first PLS component (PLS1) was identified from a gene expression profile (148 regions × 15,631 genes). A scatterplot (middle) showed the PLS1 were positively correlated with the case–control *t*-map (10,000 times permutation tests with spatial autocorrelation corrected). The PLS1 represented a transcriptional profile characterized by high expression mainly in the parietal–occipital areas but low expression in the prefrontal areas (right). (b) MDD-related genes linked to the case–control *t*-values of the primary-to-transmodal gradient. Twenty-four MDD-related genes were first identified from the Allen Human Brain Atlas dataset and 12 genes that overlapped with the 15,631 background genes were then selected. Of these, six genes were found to be significantly positively correlated with the case–control *t*-map of the primary-to-transmodal gradient (left). The *CNR1* (middle) and *CUX2* (right) gene expression showed the largest negative and positive correlation with the case–control *t*-value. $^{*}p < .05$, 10,000 times permutation tests with spatial autocorrelation and adjusted by false discovery rate. MDD, major depressive disorder; PLS1, the first partial least squares regression component.

variation, narrower gradient range, and lower gradient dispersion at global level were found. These metrics suggested that the brain network architecture of MDD patients deviated from a normal hierarchical organization toward connectivity dedifferentiation between the primary and transmodal networks. The dedifferentiated gradient pattern was complemented by excessive global integration based on graph-theoretical analysis (Figure S1). These findings were consistent with a prior study (Xia et al., 2022). All three global gradient metrics had significant correlations with greater shortest path length, smaller clustering coefficient of the brain networks, and excessive integration of the limbic network and DMN. We found significant correlations between the global gradient measurement and the HAMD scores across all patients and abnormal gradient range was also significantly correlated with the HAMA scores. Anxiety and depression symptoms are common co-occurring symptoms in MDD and subsequently contribute to increased severity and higher rates of recurrence (Hamilton et al., 2015; He et al., 2019; Li, Liu, et al., 2021). However, the underlying neurobiological substructures linking anxiety and depression symptoms in MDD patients have not yet been fully understood. Thus, we further employed mediation analysis to examine whether connectome gradient phenotype played a role in the relationship between anxiety and depression symptoms. The results indicated that the anxiety affected the depression severity via the disrupted gradient, which suggested that abnormal gradient pattern might act as an intermediate in the relationship between anxiety and depression symptoms in MDD patients. These findings had additional heuristic value for

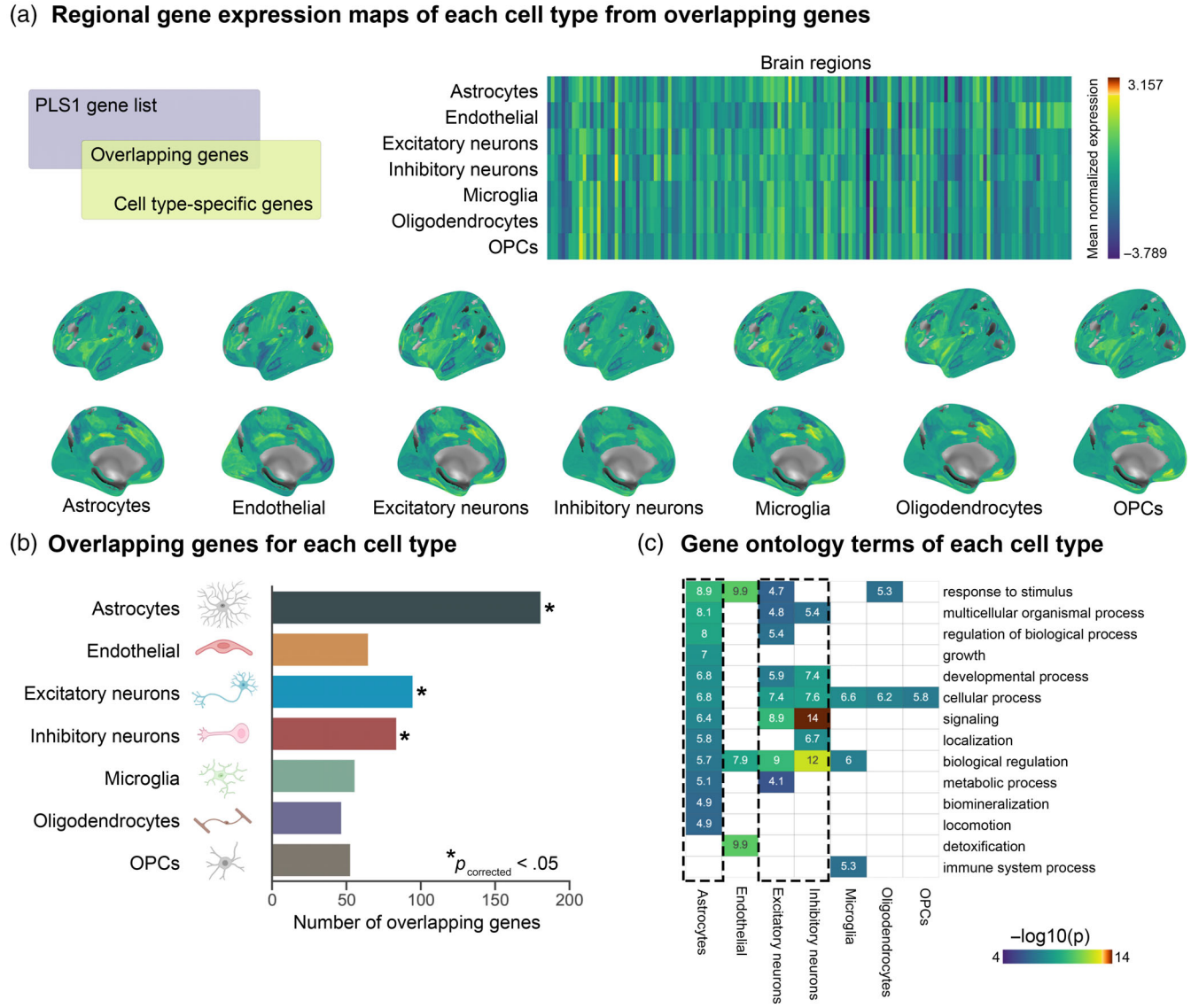

FIGURE 6 Cell type-specific gene expression to the primary-to-transmodal gradient alterations in major depressive disorder (MDD). (a) The MDD-related spatial gene expressions of seven cell types. The mean gene expression value of each region was calculated for each cell type from the PLS1− gene list and then visualized on the brain surface. (b) The number of overlapping genes for seven cell types. (c) Gene ontology terms enriched for overlapping genes of each cell type. *p < .05, 10,000 times permutation tests with spatial autocorrelation and adjusted by false discovery rate. OPCs, oligodendrocyte precursors.

understanding the origins of MDD with comorbid anxiety and its potential brain underpinnings.

The compressed primary-to-transmodal gradient in MDD was also observed at the regional level, such as MDD patients exhibiting greater gradient scores of the VIS and SMN, and lower gradient scores of the DMN. The DMN comprised cortical regions that are maximally geodesic distant from the input/output systems of the sensory and motor cortex that may support the stimulus-independence of mind-wandering (Liang et al., 2020; Scalabrini et al., 2020; Yang, Chen, et al., 2021). The DMN was linked to self-focused rumination and abnormal self-referential processes in MDD (Chen et al., 2020; Zhou et al., 2020). The maximal spatial distances between the DMN and primary network were thought to be an optimized hierarchical organization ensuring functional specialization of different brain modules (Cui et al., 2021; Yan et al., 2019; Zhou et al., 2020). The compression of the primary-to-transmodal gradient indicated excessive between-network integration or a dedifferentiation of network organization, for example the DMN undergoing degradation. Converging evidence suggested that MDD was associated with visual and sensorimotor abnormalities, as listed in the "repetitive behaviors and interests" syndrome cluster in the diagnosis criterion for MDD (Chadick & Gazzaley, 2011; Yan et al., 2019). Further studies highlighted the "sensory-first" hypothesis (Buyukdura et al., 2011; Iwabuchi et al., 2015; Snyder, 2013), which indicated that the disrupted patterns in the primary visual and SMNs were not limited to sensory-related clinical problems, but might contribute to higher-level

cognitive deficits and then these together affected network hierarchical architecture (Adams et al., 2015; Humes et al., 2013; Park, Haak, et al., 2021). We speculated that those changes in the primary systems might have cascading effects on the high-order transmodal functional systems, and this bottom-up dysregulation ultimately resulted in clinical multiple domains impairments in MDD. The findings based on subcortical-weighted manifolds complement these findings. By projecting subcortical–cortical connectivity patterns into cortical gradient space, the subcortical-weighted gradients could be used to examine parallel shifts of altered cortical gradients in subcortical regions. We found that the corresponding subcortical parallel impairments with MDD-related cortical gradient alterations were mainly located in the amygdala, thalamus, and caudate. These regions were widely interconnected with the cortex via reciprocal connections that relay and modulate cortical activity, which led to the "dysregulated interactions" hypothesis in MDD patients (Chung et al., 2011; Mayberg, 1997; Phelps & LeDoux, 2005). Our results provided consistent support that both cortical and subcortical regions can be organized together into brain networks hierarchy.

The monoamine hypothesis held that MDD was associated with abnormal function of neurotransmitters including serotonin and/or dopamine in the brain (Jiang et al., 2022; Sekiguchi et al., 2023; Sun et al., 2022). To evaluate the association between neurotransmitters and altered gradient patterns in MDD, we accessed the topographical relationship between the spatial distribution of several neurotransmitter systems and gradient-related alterations in MDD. Our results showed that the serotonin and dopamine presented a spatial association with the abnormal primary-to-transmodal gradient in MDD. It was inferred that the alterations of the brain hierarchical organization in MDD might be regulated by some microscale factors such as neurotransmitters. For example, previous studies have found that D1 receptor played an important role in regulating anxiety-like behaviors related to depression (Liang et al., 2022), while a major target of current antidepressant drugs was the serotonin system (Conio et al., 2020; Mulinari, 2012; Wainwright & Galea, 2013). Our exploratory research provided an indirect way of bridging the technology gap between changes in image phenotypes and neurotransmitter systems, which provided a microscale molecular association to account for the alterations of the primary-to-transmodal gradient in MDD. However, we associated the gradient-related changes with neurotransmitter topographies and had no information regarding neurotransmitter activity, which was previously reported as low levels in MDD (Fries et al., 2023). Future studies might seek to expand these findings based on potentially more detailed techniques.

Using gradient-transcriptome association analysis, we found a cortical spatial pattern of gene expression that was significantly correlated with MDD-related regional changes in the primary-to-transmodal gradient. This spatial distribution was consistent with a previous MDD gradient study, which exhibited high expression in the parietal–occipital regions and low expression in the prefrontal regions (Xia et al., 2022). Correlation analysis with MDD-related risk genes showed that 6 of 12 risk genes were related to abnormal primary-transmodal gradient. Therein, the *CNR1* gene showed the greatest negative correlation and its high expression was located mainly in the medial prefrontal areas. The *CUX2* gene exhibited the greatest positive correlation and high expression in the primary sensory and visual cortex. As a key component of the endocannabinoid system, the *CNR1* contributed to the support of the molecular architecture of processing reward and perception of certain basic emotions, and was even regarded as a promising genetic predictor for diagnosis of MDD and treatment response to antidepressants (Icick et al., 2015; Yang, Nolte, et al., 2021; Yao et al., 2018). For example, previous research has shown that variations in *CNR1* modulated the striatal response to emotional faces (Anderson, Collins, Chin, et al., 2020; Mecca et al., 2021; Tsuboi et al., 2022). Similar to *CNR1*, the *CUX2* was also a gene earlier noted to be a candidate gene for MDD and related to multiple functions and activity of neurons (Abbass et al., 2018; Ma et al., 2022). Notably, we did not have accessed to the gene expression characteristics of our samples. Our findings just suggested that the spatial alignment between MDD-related aberrant gradient pattern and gene expression from AHBA donors was broadly similar, which might limit the ability to determine the effects of genetic variations on abnormal gradient patterns (Romero-Garcia et al., 2019). Within-subject studies assessing the relationship between genetic and neuroimaging data will be needed.

We conducted cell type-specific characterization of the gradient-related genes to assess which cell types might engender selective brain gradient changes in MDD. Our findings indicated that the MDD-related gradient alteration was associated with genes expressed primarily in astrocytes and neurons. Astrocytes are generally recognized to play supporting roles in the brain, yet emerging researches have pointed out more direct roles of astrocytes for brain functions (Fee et al., 2017; Rajkowska & Stockmeier, 2013; Tripp et al., 2011). For example, much evidence from rodent models indicated that astrocytes could not only detect serotonin and noradrenaline in synaptic transmission, but also uptaked these neurotransmitters (Guo et al., 2022; Portal et al., 2022; Zhang et al., 2023). The mechanism of astrocytes involvement in MDD was thought to be through influencing synaptic activity and modulating neuronal circuits, such as an imbalance between excitatory and inhibitory neurons (Anderson, Collins, Chin, et al., 2020; Li, Seidlitz, et al., 2021). Enrichment analysis of gradient-related cell-types specific genes showed that the most enriched pathway was also primarily in biological processes of astrocytes and neurons, suggesting the observed cell types associated with gradient changes might directly arise through genetic factors tied to risk variants of genes in identifying several cells. Our new findings helped us to understand the key role of cell type-specific gene expression in MDD-related gradient compression.

Several issues need to be considered. First, the present sample derived from the REST-meta-MDD Project did not have complete clinical information, such as treatment response and duration of illness. More than one third of patients had no information about whether they are medication-experienced patients in current data. Although our further analysis found that there was no statistically significant case–control gradient difference between the patients with and without medication, future studies should include more comprehensive

metrics to examine possible effects from various MDD-related clinical variables. Second, patients and controls were not matched by years of education in the present sample. Alternatively, we controlled the effect of education level as a covariate in the comparison analyses. Future study should choose the matching participants to reduce its influence. Third, the choice of the applied atlas in performing spatial correlation may impact our findings. In the present study, we used Zalesky's atlas to anatomically parcellate the human cerebral cortex into 980 similar-sized brain regions (Zalesky et al., 2010). The atlas was widely used to measure the topological properties of the cerebral cortex networks in both morphometric and functional studies (Dai et al., 2019; Tzourio-Mazoyer et al., 2002), and the efficacy and reliability of functional gradients in a recent study (Zhang & Zang, 2023). Another study used this atlas to measure the relationship between cortical functional attributes and gene expression profiles from the AHBA (Li, Wei, et al., 2021). Further studies should be conducted to evaluate the effects of the choice of atlas on the present results. Fourth, the gene data from the AHBA dataset was measured from postmortem brain tissue of five healthy male donors and one healthy female donor that did not fully capture the individual variation of gene expression in the cortex. The neuroimaging-transcriptome association analysis is based on a hypothesis that cortical gene expression patterns are highly conserved across individuals (Hawrylycz et al., 2015). Some genes that are not sufficiently conserved across individuals may be missed and the statistical power of identified related genes may be reduced in such analysis, which need to be taken into consideration while interpreting these results. Fifth, gene expression data processing may impact imaging-genetic results (Arnatkeviciute et al., 2019). We preprocessed the gene expression microarray data by using a well-done proposed standardized pipeline which is based on a systematic assessment of the workflow combining AHBA and neuroimaging data (Martins et al., 2021; Zhao et al., 2022). Despite these procedures, the influence from different processing choices remained, and may furthermore require additional caution in interpreting our findings. The gene expression data from MDD patients was necessary for further verifying the relationship between gradient-related changes and its gene expression. Finally, we used spatial correlation to chart microscale neurotransmitters and cellular signatures relating to the macroscale alteration of functional gradient in MDD, which yielded suggestive associations but demonstration of genetic causative disease role required direct interventions. Therefore, our study was an exploratory associated study, aiming at providing inspiration for informing prognosis and guiding treatment. Future work of combining spatial genome with individual-specific transcriptomic profiling will deepen our understanding of pathophysiology in MDD.

5 | CONCLUSIONS

In summary, this study delineated a compressed primary-to-transmdodal gradient in MDD patients and linked it to other macroscale neuroimaging indexes and potential microscale neurobiological characteristics. We found that alterations in subcortical gradients involved the cortical gradient reconfiguration and paralleled subcortical impairments were found in caudate, amygdala, and thalamus. In addition, gradient-related differences were associated with dopaminergic and serotonergic systems, as well as cell type-specific transcriptional signatures including astrocytes and neurons. These findings were a step forward in an integrative understanding of MDD-related co-deficits of sensory and cognitive in MDD patients with convergent neurotransmitter and cellular signatures which are related to the impairments of hierarchical organization.

ACKNOWLEDGMENTS

This work was supported by the Natural Science Foundation of Zhejiang Province (LY17H180007), Key Medical Disciplines of Hangzhou, Zhejiang Medical and Health Science and Technology Project (2022490271), and Affiliated Hospital of Hangzhou Normal University (2021YN2021105, KY21085). The authors would like to thank Prof. Xi-Nian Zuo for his insightful comments and Prof. Hong Luo and Zhiguo Hu for their help with this work. The authors thank the DIRECT consortium for collecting and sharing the data.

CONFLICT OF INTEREST STATEMENT

The authors report no biomedical financial interests or potential conflicts of interest.

DATA AVAILABILITY STATEMENT

The dataset of participants is available through a reasonable request to the Rest-meta-MDD consortium (http://rfmri.org/REST-meta-MDD). All PET maps of neurotransmitters are derived from the JuSpace toolbox (https://github.com/juryxy/JuSpace), and transcriptomic data from the Allen human brain atlas (https://human.brain-map.org/). The codes for generating connectome gradient are available at BrainSpace (https://github.com/MICA-MNI/BrainSpace).

ORCID

Yang Xiao https://orcid.org/0000-0002-9746-9571
Lei Zhao https://orcid.org/0000-0002-6418-7201
Shao-Wei Xue https://orcid.org/0000-0001-5441-4522

REFERENCES

Abbass, M., Trought, K., Long, D., Semechko, A., & Wong, A. H. C. (2018). Automated immunohistochemical method to analyze large areas of the human cortex. *Journal of Neuroscience Methods*, *294*, 81–90. https://doi.org/10.1016/j.jneumeth.2017.10.024

Adams, J. N., Feldman, H. M., Huffman, L. C., & Loe, I. M. (2015). Sensory processing in preterm preschoolers and its association with executive function. *Early Human Development*, *91*(3), 227–233. https://doi.org/10.1016/j.earlhumdev.2015.01.013

Anderson, K. M., Collins, M. A., Chin, R., Ge, T., Rosenberg, M. D., & Holmes, A. J. (2020). Transcriptional and imaging-genetic association of cortical interneurons, brain function, and schizophrenia risk. *Nature Communications*, *11*(1), 2889. https://doi.org/10.1038/s41467-020-16710-x

Anderson, K. M., Collins, M. A., Kong, R., Fang, K., Li, J., He, T., Chekroud, A. M., Thomas Yeo, B. T., & Holmes, A. J. (2020). Convergent molecular, cellular, and cortical neuroimaging signatures of major depressive disorder. *Proceedings of the National Academy of Sciences of the United States of America*, *117*(40), 25138–25149. https://doi.org/10.1073/pnas.2008004117

Arnatkeviciute, A., Fulcher, B. D., & Fornito, A. (2019). A practical guide to linking brain-wide gene expression and neuroimaging data. *NeuroImage*, *189*, 353–367. https://doi.org/10.1016/j.neuroimage.2019.01.011

Bubl, E., Kern, E., Ebert, D., Bach, M., & Tebartz van Elst, L. (2010). Seeing gray when feeling blue? Depression can be measured in the eye of the diseased. *Biological Psychiatry*, *68*(2), 205–208. https://doi.org/10.1016/j.biopsych.2010.02.009

Buyukdura, J. S., McClintock, S. M., & Croarkin, P. E. (2011). Psychomotor retardation in depression: Biological underpinnings, measurement, and treatment. *Progress in Neuro-Psychopharmacology & Biological Psychiatry*, *35*(2), 395–409. https://doi.org/10.1016/j.pnpbp.2010.10.019

Chadick, J. Z., & Gazzaley, A. (2011). Differential coupling of visual cortex with default or frontal-parietal network based on goals. *Nature Neuroscience*, *14*(7), 830–832. https://doi.org/10.1038/nn.2823

Chen, J., Müller, V. I., Dukart, J., Hoffstaedter, F., Baker, J. T., Holmes, A. J., Vatansever, D., Nickl-Jockschat, T., Liu, X., Derntl, B., Kogler, L., Jardri, R., Gruber, O., Aleman, A., Sommer, I. E., Eickhoff, S. B., & Patil, K. R. (2021). Intrinsic connectivity patterns of task-defined brain networks allow individual prediction of cognitive symptom dimension of schizophrenia and are linked to molecular architecture. *Biological Psychiatry*, *89*(3), 308–319. https://doi.org/10.1016/j.biopsych.2020.09.024

Chen, X., Chen, N. X., Shen, Y. Q., Li, H. X., Li, L., Lu, B., Fan, Z., Yan, C. G., & Yan, C. G. (2020). The subsystem mechanism of default mode network underlying rumination: A reproducible neuroimaging study. *NeuroImage*, *221*, 117185. https://doi.org/10.1016/j.neuroimage.2020.117185

Chen, X., Lu, B., Li, H.-X., Li, X.-Y., Wang, Y.-W., Castellanos, F. X., Cao, L. P., Chen, N. X., Chen, W., Cheng, Y. Q., Cui, S. X., Deng, Z. Y., Fang, Y. R., Gong, Q. Y., Guo, W. B., Hu, Z. J. Y., Kuang, L., Li, B. J., Li, L., … Yan, C.-G. (2022). The DIRECT consortium and the REST-meta-MDD project: Towards neuroimaging biomarkers of major depressive disorder. *Psychoradiology*, *2*(1), 32–42. https://doi.org/10.1093/psyrad/kkac005

Chung, Y. S., Mathews, J. R., & Barch, D. M. (2011). The effect of context processing on different aspects of social cognition in schizophrenia. *Schizophrenia Bulletin*, *37*(5), 1048–1056. https://doi.org/10.1093/schbul/sbq012

Conio, B., Martino, M., Magioncalda, P., Escelsior, A., Inglese, M., Amore, M., & Northoff, G. (2020). Opposite effects of dopamine and serotonin on resting-state networks: Review and implications for psychiatric disorders. *Molecular Psychiatry*, *25*(1), 82–93. https://doi.org/10.1038/s41380-019-0406-4

Cui, J., Wang, Y., Liu, R., Chen, X., Zhang, Z., Feng, Y., Zhou, J., Zhou, Y., & Wang, G. (2021). Effects of escitalopram therapy on resting-state functional connectivity of subsystems of the default mode network in unmedicated patients with major depressive disorder. *Translational Psychiatry*, *11*(1), 634. https://doi.org/10.1038/s41398-021-01754-4

Dai, Z., Lin, Q., Li, T., Wang, X., Yuan, H., Yu, X., He, Y., & Wang, H. (2019). Disrupted structural and functional brain networks in Alzheimer's disease. *Neurobiology of Aging*, *75*, 71–82. https://doi.org/10.1016/j.neurobiolaging.2018.11.005

Di Biase, M. A., Geaghan, M. P., Reay, W. R., Seidlitz, J., Weickert, C. S., Pébay, A., Green, M. J., Quidé, Y., Atkins, J. R., Coleman, M. J., Bouix, S., Knyazhanskaya, E. E., Lyall, A. E., Pasternak, O., Kubicki, M., Rathi, Y., Visco, A., Gaunnac, M., Lv, J., … Zalesky, A. (2022). Cell type-specific manifestations of cortical thickness heterogeneity in schizophrenia. *Molecular Psychiatry*, *27*(4), 2052–2060. https://doi.org/10.1038/s41380-022-01460-7

Drysdale, A. T., Grosenick, L., Downar, J., Dunlop, K., Mansouri, F., Meng, Y., Fetcho, R. N., Zebley, B., Oathes, D. J., Etkin, A., Schatzberg, A. F., Sudheimer, K., Keller, J., Mayberg, H. S., Gunning, F. M., Alexopoulos, G. S., Fox, M. D., Pascual-Leone, A., Voss, H. U., … Liston, C. (2017). Resting-state connectivity biomarkers define neurophysiological subtypes of depression. *Nature Medicine*, *23*(1), 28–38. https://doi.org/10.1038/nm.4246

Dukart, J., Holiga, S., Rullmann, M., Lanzenberger, R., Hawkins, P. C. T., Mehta, M. A., Hesse, S., Barthel, H., Sabri, O., Jech, R., & Eickhoff, S. B. (2021). JuSpace: A tool for spatial correlation analyses of magnetic resonance imaging data with nuclear imaging derived neurotransmitter maps. *Human Brain Mapping*, *42*(3), 555–566. https://doi.org/10.1002/hbm.25244

Elman, J. A., Panizzon, M. S., Hagler, D. J., Jr., Fennema-Notestine, C., Eyler, L. T., Gillespie, N. A., Neale, M. C., Lyons, M. J., Franz, C. E., McEvoy, L. K., Dale, A. M., & Kremen, W. S. (2017). Genetic and environmental influences on cortical mean diffusivity. *NeuroImage*, *146*, 90–99. https://doi.org/10.1016/j.neuroimage.2016.11.032

Fee, C., Banasr, M., & Sibille, E. (2017). Somatostatin-positive gamma-aminobutyric acid interneuron deficits in depression: Cortical microcircuit and therapeutic perspectives. *Biological Psychiatry*, *82*(8), 549–559. https://doi.org/10.1016/j.biopsych.2017.05.024

Fitzgerald, P. J. (2013). Gray colored glasses: Is major depression partially a sensory perceptual disorder? *Journal of Affective Disorders*, *151*(2), 418–422. https://doi.org/10.1016/j.jad.2013.06.045

Fornito, A., Arnatkevičiūtė, A., & Fulcher, B. D. (2019). Bridging the gap between connectome and transcriptome. *Trends in Cognitive Sciences*, *23*(1), 34–50. https://doi.org/10.1016/j.tics.2018.10.005

Fries, G. R., Saldana, V. A., Finnstein, J., & Rein, T. (2023). Molecular pathways of major depressive disorder converge on the synapse. *Molecular Psychiatry*, *28*(1), 284–297. https://doi.org/10.1038/s41380-022-01806-1

Greene, D. J., Marek, S., Gordon, E. M., Siegel, J. S., Gratton, C., Laumann, T. O., Gilmore, A. W., Berg, J. F., Nguyen, A. L., Dierker, D., Van, A. N., Ortega, M., Newbold, D. J., Hampton, J. M., Nielsen, A. N., McDermott, K. B., Roland, J. L., Norris, S. A., Nelson, S. M., … Dosenbach, N. U. F. (2020). Integrative and network-specific connectivity of the basal ganglia and thalamus defined in individuals. *Neuron*, *105*(4), 742–758.e746. https://doi.org/10.1016/j.neuron.2019.11.012

Guo, A., Zhang, H., Li, H., Chiu, A., García-Rodríguez, C., Lagos, C. F., Sáez, J. C., & Lau, C. G. (2022). Inhibition of connexin hemichannels alleviates neuroinflammation and hyperexcitability in temporal lobe epilepsy. *Proceedings of the National Academy of Sciences of the United States of America*, *119*(45), e2213162119. https://doi.org/10.1073/pnas.2213162119

Haak, K. V., & Beckmann, C. F. (2020). Understanding brain organisation in the face of functional heterogeneity and functional multiplicity. *NeuroImage*, *220*, 117061. https://doi.org/10.1016/j.neuroimage.2020.117061

Hamilton, J. P., Chen, M. C., Waugh, C. E., Joormann, J., & Gotlib, I. H. (2015). Distinctive and common neural underpinnings of major depression, social anxiety, and their comorbidity. *Social Cognitive and Affective Neuroscience*, *10*(4), 552–560. https://doi.org/10.1093/scan/nsu084

Haueis, P. (2021). Multiscale modeling of cortical gradients: The role of mesoscale circuits for linking macro- and microscale gradients of cortical organization and hierarchical information processing. *NeuroImage*, *232*, 117846. https://doi.org/10.1016/j.neuroimage.2021.117846

Hawrylycz, M., Miller, J. A., Menon, V., Feng, D., Dolbeare, T., Guillozet-Bongaarts, A. L., Jegga, A. G., Aronow, B. J., Lee, C. K., Bernard, A., Glasser, M. F., Dierker, D. L., Menche, J., Szafer, A., Collman, F., Grange, P., Berman, K. A., Mihalas, S., Yao, Z., … Lein, E. (2015). Canonical genetic signatures of the adult human brain. *Nature Neuroscience*, *18*(12), 1832–1844. https://doi.org/10.1038/nn.4171

He, C., Gong, L., Yin, Y., Yuan, Y., Zhang, H., Lv, L., Zhang, X., Soares, J. C., Zhang, H., Xie, C., & Zhang, Z. (2019). Amygdala connectivity mediates the association between anxiety and depression in patients with major depressive disorder. *Brain Imaging and Behavior*, *13*(4), 1146–1159. https://doi.org/10.1007/s11682-018-9923-z

Hesse, S., Becker, G. A., Rullmann, M., Bresch, A., Luthardt, J., Hankir, M. K., Zientek, F., Reißig, G., Patt, M., Arelin, K., Lobsien, D., Müller, U., Baldofski, S., Meyer, P. M., Blüher, M., Fasshauer, M., Fenske, W. K., Stumvoll, M., Hilbert, A., … Sabri, O. (2017). Central noradrenaline transporter availability in highly obese, non-depressed individuals. *European Journal of Nuclear Medicine and Molecular Imaging*, *44*(6), 1056–1064. https://doi.org/10.1007/s00259-016-3590-3

Hibar, D. P., Stein, J. L., Renteria, M. E., Arias-Vasquez, A., Desrivières, S., Jahanshad, N., Roberto Toro, R., Wittfeld, K., Abramovic, L., Andersson, M., Aribisala, B. S., Armstrong, N. J., Bernard, M., Bohlken, M. M., Boks, M. P., Bralten, J., Brown, A. A., Chakravarty, M. M., Chen, Q., … Medland, S. E. (2015). Common genetic variants influence human subcortical brain structures. *Nature*, *520*(7546), 224–229. https://doi.org/10.1038/nature14101

Hong, S. J., Vos de Wael, R., Bethlehem, R. A. I., Lariviere, S., Paquola, C., Valk, S. L., Milham, M. P., Di Martino, A., Margulies, D. S., Smallwood, J., & Bernhardt, B. C. (2019). Atypical functional connectome hierarchy in autism. *Nature Communications*, *10*(1), 1022. https://doi.org/10.1038/s41467-019-08944-1

Humes, L. E., Busey, T. A., Craig, J., & Kewley-Port, D. (2013). Are age-related changes in cognitive function driven by age-related changes in sensory processing? *Attention, Perception, & Psychophysics*, *75*(3), 508–524. https://doi.org/10.3758/s13414-012-0406-9

Huntenburg, J. M., Bazin, P. L., Goulas, A., Tardif, C. L., Villringer, A., & Margulies, D. S. (2017). A systematic relationship between functional connectivity and intracortical myelin in the human cerebral cortex. *Cerebral Cortex*, *27*(2), 981–997. https://doi.org/10.1093/cercor/bhx030

Huntenburg, J. M., Bazin, P. L., & Margulies, D. S. (2018). Large-scale gradients in human cortical organization. *Trends in Cognitive Sciences*, *22*(1), 21–31. https://doi.org/10.1016/j.tics.2017.11.002

Icick, R., Peoc'h, K., Karsinti, E., Ksouda, K., Hajj, A., Bloch, V., Prince, N., Mouly, S., Bellivier, F., Lépine, J. P., Laplanche, J. L., & Vorspan, F. (2015). A cannabinoid receptor 1 polymorphism is protective against major depressive disorder in methadone-maintained outpatients. *The American Journal on Addictions*, *24*(7), 613–620. https://doi.org/10.1111/ajad.12273

Iwabuchi, S. J., Krishnadas, R., Li, C., Auer, D. P., Radua, J., & Palaniyappan, L. (2015). Localized connectivity in depression: A meta-analysis of resting state functional imaging studies. *Neuroscience and Biobehavioral Reviews*, *51*, 77–86. https://doi.org/10.1016/j.neubiorev.2015.01.006

Jiang, Y., Zou, D., Li, Y., Gu, S., Dong, J., Ma, X., Xu, S., Wang, F., & Huang, J. H. (2022). Monoamine neurotransmitters control basic emotions and affect major depressive disorders. *Pharmaceuticals (Basel)*, *15*(10), 1203. https://doi.org/10.3390/ph15101203

Kaller, S., Rullmann, M., Patt, M., Becker, G. A., Luthardt, J., Girbardt, J., Meyer, P. M., Werner, P., Barthel, H., McLeod, A., Fritz, T., & Sabri, O. (2017). Test–retest measurements of dopamine D(1)-type receptors using simultaneous PET/MRI imaging. *European Journal of Nuclear Medicine and Molecular Imaging*, *44*(6), 1025–1032. https://doi.org/10.1007/s00259-017-3645-0

Kennedy, D. N., Lange, N., Makris, N., Bates, J., Meyer, J., & Caviness, V. S., Jr. (1998). Gyri of the human neocortex: An MRI-based analysis of volume and variance. *Cerebral Cortex*, *8*(4), 372–384. https://doi.org/10.1093/cercor/8.4.372

Li, G., Liu, Y., Zheng, Y., Wu, Y., Li, D., Liang, X., Chen, Y., Cui, Y., Yap, P. T., Qiu, S., Zhang, H., & Shen, D. (2021). Multiscale neural modeling of resting-state fMRI reveals executive-limbic malfunction as a core mechanism in major depressive disorder. *Neuroimage Clinical*, *31*, 102758. https://doi.org/10.1016/j.nicl.2021.102758

Li, J., Seidlitz, J., Suckling, J., Fan, F., Ji, G. J., Meng, Y., Yang, S., Wang, K., Qiu, J., Chen, H., & Liao, W. (2021). Cortical structural differences in major depressive disorder correlate with cell type-specific transcriptional signatures. *Nature Communications*, *12*(1), 1647. https://doi.org/10.1038/s41467-021-21943-5

Li, L., Wei, Y., Zhang, J., Ma, J., Yi, Y., Gu, Y., Li, L. M. W., Lin, Y., & Dai, Z. (2021). Gene expression associated with individual variability in intrinsic functional connectivity. *NeuroImage*, *245*, 118743. https://doi.org/10.1016/j.neuroimage.2021.118743

Liang, S., Wu, Y., Hanxiaoran, L., Greenshaw, A. J., & Li, T. (2022). Anhedonia in depression and schizophrenia: Brain reward and aversion circuits. *Neuropsychiatric Disease and Treatment*, *18*, 1385–1396. https://doi.org/10.2147/ndt.S367839

Liang, Y., Yao, Y. C., Zhao, L., Shi, L., Chen, Y. K., Mok, V. C., Ungvari, G. S., Chu, W. C., & Tang, W. K. (2020). Topological reorganization of the default mode network in patients with poststroke depressive symptoms: A resting-state fMRI study. *Journal of Affective Disorders*, *260*, 557–568. https://doi.org/10.1016/j.jad.2019.09.051

Ma, N. X., Puls, B., & Chen, G. (2022). Transcriptomic analyses of NeuroD1-mediated astrocyte-to-neuron conversion. *Developmental Neurobiology*, *82*(5), 375–391. https://doi.org/10.1002/dneu.22882

Malhotra, A. K., Goldman, D., Mazzanti, C., Clifton, A., Breier, A., & Pickar, D. (1998). A functional serotonin transporter (5-HTT) polymorphism is associated with psychosis in neuroleptic-free schizophrenics. *Molecular Psychiatry*, *3*(4), 328–332. https://doi.org/10.1038/sj.mp.4000412

Margulies, D. S., Ghosh, S. S., Goulas, A., Falkiewicz, M., Huntenburg, J. M., Langs, G., Bezgin, G., Eickhoff, S. B., Xavier Castellanos, F., Petrides, M., Jefferies, E., & Smallwood, J. (2016). Situating the default-mode network along a principal gradient of macroscale cortical organization. *Proceedings of the National Academy of Sciences of the United States of America*, *113*(44), 12574–12579. https://doi.org/10.1073/pnas.1608282113

Martins, D., Giacomel, A., Williams, S. C. R., Turkheimer, F., Dipasquale, O., & Veronese, M. (2021). Imaging transcriptomics: Convergent cellular, transcriptomic, and molecular neuroimaging signatures in the healthy adult human brain. *Cell Reports*, *37*(13), 110173. https://doi.org/10.1016/j.celrep.2021.110173

Mayberg, H. S. (1997). Limbic-cortical dysregulation: A proposed model of depression. *The Journal of Neuropsychiatry and Clinical Neurosciences*, *9*(3), 471–481. https://doi.org/10.1176/jnp.9.3.471

Mecca, C. M., Chao, D., Yu, G., Feng, Y., Segel, I., Zhang, Z., Rodriguez-Garcia, D. M., Pawela, C. P., Hillard, C. J., Hogan, Q. H., & Pan, B. (2021). Dynamic change of endocannabinoid signaling in the medial prefrontal cortex controls the development of depression after neuropathic pain. *The Journal of Neuroscience*, *41*(35), 7492–7508. https://doi.org/10.1523/jneurosci.3135-20.2021

Mulinari, S. (2012). Monoamine theories of depression: Historical impact on biomedical research. *Journal of the History of the Neurosciences*, *21*(4), 366–392. https://doi.org/10.1080/0964704x.2011.623917

Park, B. Y., Bethlehem, R. A., Paquola, C., Larivière, S., Rodríguez-Cruces, R., Vos de Wael, R., Neuroscience in Psychiatry Network (NSPN) Consortium, Bullmore, E. T., & Bernhardt, B. C. (2021). An expanding manifold in transmodal regions characterizes adolescent reconfiguration of structural connectome organization. *eLife*, *10*, e64694. https://doi.org/10.7554/eLife.64694

Park, B. Y., Hong, S. J., Valk, S. L., Paquola, C., Benkarim, O., Bethlehem, R. A. I., Di Martino, A., Milham, M. P., Gozzi, A., Thomas Yeo, B. T., Smallwood, J., & Bernhardt, B. C. (2021). Differences in subcortico-cortical interactions identified from connectome and microcircuit models in autism. *Nature Communications*, *12*(1), 2225. https://doi.org/10.1038/s41467-021-21732-0

Park, B. Y., Kebets, V., Larivière, S., Hettwer, M. D., Paquola, C., van Rooij, D., Buitelaar, J., Franke, B., Hoogman, M., Schmaal, L., Veltman, D. J., van den Heuvel, O. A., Stein, D. J., Andreassen, O. A., Ching, C. R. K., Turner, J. A., van Erp, T. G. M., Evans, A. C., Dagher, A., … Bernhardt, B. C. (2022). Multiscale neural gradients reflect

transdiagnostic effects of major psychiatric conditions on cortical morphology. *Communications Biology*, *5*(1), 1024. https://doi.org/10.1038/s42003-022-03963-z

Park, S., Haak, K. V., Cho, H. B., Valk, S. L., Bethlehem, R. A. I., Milham, M. P., Bernhardt, B. C., Di Martino, A., & Hong, S. J. (2021). Atypical integration of sensory-to-transmodal functional systems mediates symptom severity in autism. *Frontiers in Psychiatry*, *12*, 699813. https://doi.org/10.3389/fpsyt.2021.699813

Phelps, E. A., & LeDoux, J. E. (2005). Contributions of the amygdala to emotion processing: From animal models to human behavior. *Neuron*, *48*(2), 175–187. https://doi.org/10.1016/j.neuron.2005.09.025

Portal, B., Vasile, F., Zapata, J., Lejards, C., Ait Tayeb, A. E. K., Colle, R., Verstuyft, C., Corruble, E., Rouach, N., & Guiard, B. P. (2022). Astroglial connexins inactivation increases relapse of depressive-like phenotype after antidepressant withdrawal. *International Journal of Molecular Sciences*, *23*(21), 13227. https://doi.org/10.3390/ijms232113227

Rajkowska, G., & Stockmeier, C. A. (2013). Astrocyte pathology in major depressive disorder: Insights from human postmortem brain tissue. *Current Drug Targets*, *14*(11), 1225–1236. https://doi.org/10.2174/13894501131499990156

Romero-Garcia, R., Warrier, V., Bullmore, E. T., Baron-Cohen, S., & Bethlehem, R. A. I. (2019). Synaptic and transcriptionally downregulated genes are associated with cortical thickness differences in autism. *Molecular Psychiatry*, *24*(7), 1053–1064. https://doi.org/10.1038/s41380-018-0023-7

Scalabrini, A., Vai, B., Poletti, S., Damiani, S., Mucci, C., Colombo, C., Zanardi, R., Benedetti, F., & Northoff, G. (2020). All roads lead to the default-mode network-global source of DMN abnormalities in major depressive disorder. *Neuropsychopharmacology*, *45*(12), 2058–2069. https://doi.org/10.1038/s41386-020-0785-x

Seidlitz, J., Nadig, A., Liu, S., Bethlehem, R. A. I., Vértes, P. E., Morgan, S. E., Váša, F., Romero-Garcia, R., Lalonde, F. M., Clasen, L. S., Blumenthal, J. D., Paquola, C., Bernhardt, B., Wagstyl, K., Polioudakis, D., de la Torre-Ubieta, L., Geschwind, D. H., Han, J. C., Lee, N. R., … Raznahan, A. (2020). Transcriptomic and cellular decoding of regional brain vulnerability to neurogenetic disorders. *Nature Communications*, *11*(1), 3358. https://doi.org/10.1038/s41467-020-17051-5

Sekiguchi, H., Pavey, G., & Dean, B. (2023). Altered levels of dopamine transporter in the frontal pole and the striatum in mood disorders: A postmortem study. *Journal of Affective Disorders*, *320*, 313–318. https://doi.org/10.1016/j.jad.2022.09.065

Sepulcre, J., Sabuncu, M. R., Yeo, T. B., Liu, H., & Johnson, K. A. (2012). Stepwise connectivity of the modal cortex reveals the multimodal organization of the human brain. *The Journal of Neuroscience*, *32*(31), 10649–10661. https://doi.org/10.1523/jneurosci.0759-12.2012

Siegel, J. S., Snyder, A. Z., Metcalf, N. V., Fucetola, R. P., Hacker, C. D., Shimony, J. S., Shulman, G. L., & Corbetta, M. (2014). The circuitry of abulia: Insights from functional connectivity MRI. *Neuroimage Clinical*, *6*, 320–326. https://doi.org/10.1016/j.nicl.2014.09.012

Snyder, H. R. (2013). Major depressive disorder is associated with broad impairments on neuropsychological measures of executive function: A meta-analysis and review. *Psychological Bulletin*, *139*(1), 81–132. https://doi.org/10.1037/a0028727

Sun, N., Qin, Y. J., Xu, C., Xia, T., Du, Z. W., Zheng, L. P., An-An Li, A. A., Meng, F., Zhang, Y., Zhang, J., Liu, X., Li, T. Y., Zhu, D. Y., & Zhou, Q. G. (2022). Design of fast-onset antidepressant by dissociating SERT from nNOS in the DRN. *Science*, *378*(6618), 390–398. https://doi.org/10.1126/science.abo3566

Tripp, A., Kota, R. S., Lewis, D. A., & Sibille, E. (2011). Reduced somatostatin in subgenual anterior cingulate cortex in major depression. *Neurobiology of Disease*, *42*(1), 116–124. https://doi.org/10.1016/j.nbd.2011.01.014

Tsuboi, H., Matsunaga, M., Tsujiguchi, H., Kannon, T., Hosomichi, K., Sato, T., Tajima, A., Yoshida, N., Hara, A., & Nakamura, H. (2022). Elevated ratio of serum anandamide to arachidonic acid intake in community-dwelling women with high depressive symptoms. *Neuro Endocrinology Letters*, *43*(3), 145–153.

Tzourio-Mazoyer, N., Landeau, B., Papathanassiou, D., Crivello, F., Etard, O., Delcroix, N., Mazoyer, B., & Joliot, M. (2002). Automated anatomical labeling of activations in SPM using a macroscopic anatomical parcellation of the MNI MRI single-subject brain. *NeuroImage*, *15*(1), 273–289. https://doi.org/10.1006/nimg.2001.0978

Wainwright, S. R., & Galea, L. A. (2013). The neural plasticity theory of depression: Assessing the roles of adult neurogenesis and PSA-NCAM within the hippocampus. *Neural Plasticity*, *2013*, 805497. https://doi.org/10.1155/2013/805497

Xia, M., Liu, J., Mechelli, A., Sun, X., Ma, Q., Wang, X., Wei, D., Chen, Y., Liu, B., Huang, C. C., Zheng, Y., Wu, Y., Chen, T., Cheng, Y., Xu, X., Gong, Q., Si, T., Qiu, S., Lin, C. P., … He, Y. (2022). Connectome gradient dysfunction in major depression and its association with gene expression profiles and treatment outcomes. *Molecular Psychiatry*, *27*(3), 1384–1393. https://doi.org/10.1038/s41380-022-01519-5

Yan, C. G., Chen, X., Li, L., Castellanos, F. X., Bai, T. J., Bo, Q. J., Cao, J., Chen, G. M., Chen, N. X., Chen, W., Cheng, C., Cheng, Y. Q., Cui, X. L., Duan, J., Fang, Y. R., Gong, Q. Y., Guo, W. B., Hou, Z. H., Hu, L., … Zang, Y. F. (2019). Reduced default mode network functional connectivity in patients with recurrent major depressive disorder. *Proceedings of the National Academy of Sciences of the United States of America*, *116*(18), 9078–9083. https://doi.org/10.1073/pnas.1900390116

Yang, C., Nolte, I. M., Ma, Y., An, X., Bosker, F. J., & Li, J. (2021). The associations of CNR1 SNPs and haplotypes with vulnerability and treatment response phenotypes in Han Chinese with major depressive disorder: A case-control association study. *Molecular Genetics & Genomic Medicine*, *9*(9), e1752. https://doi.org/10.1002/mgg3.1752

Yang, H., Chen, X., Chen, Z. B., Li, L., Li, X. Y., Castellanos, F. X., Bai, T. J., Bo, Q. J., Cao, J., Chang, Z. K., Chen, G. M., Chen, N. X., Chen, W., Cheng, C., Cheng, Y. Q., Cui, X. L., Duan, J., Fang, Y., Gong, Q. Y., … Yan, C. G. (2021). Disrupted intrinsic functional brain topology in patients with major depressive disorder. *Molecular Psychiatry*, *26*(12), 7363–7371. https://doi.org/10.1038/s41380-021-01247-2

Yao, Y., Xu, Y., Zhao, J., Ma, Y., Su, K., Yuan, W., Ma, J. Z., Payne, T. J., & Li, M. D. (2018). Detection of significant association between variants in cannabinoid receptor 1 gene (CNR1) and personality in African-American population. *Frontiers in Genetics*, *9*, 199. https://doi.org/10.3389/fgene.2018.00199

Yeo, B. T., Krienen, F. M., Sepulcre, J., Sabuncu, M. R., Lashkari, D., Hollinshead, M., Roffman, J. L., Smoller, J. W., Zöllei, L., Polimeni, J. R., Fischl, B., Liu, H., & Buckner, R. L. (2011). The organization of the human cerebral cortex estimated by intrinsic functional connectivity. *Journal of Neurophysiology*, *106*(3), 1125–1165. https://doi.org/10.1152/jn.00338.2011

Yu, M., Linn, K. A., Cook, P. A., Phillips, M. L., McInnis, M., Fava, M., Trivedi, M. H., Weissman, M. M., Shinohara, R., & Sheline, Y. I. (2018). Statistical harmonization corrects site effects in functional connectivity measurements from multi-site fMRI data. *Human Brain Mapping*, *39*(11), 4213–4227. https://doi.org/10.1002/hbm.24241

Zalesky, A., Fornito, A., Harding, I. H., Cocchi, L., Yücel, M., Pantelis, C., & Bullmore, E. T. (2010). Whole-brain anatomical networks: Does the choice of nodes matter? *NeuroImage*, *50*(3), 970–983. https://doi.org/10.1016/j.neuroimage.2009.12.027

Zhang, J. X., Zhou, K. G., Yin, Y. X., Jin, L. J., Tong, W. F., Guo, J., Yu, L. H., Ye, X. C., & Jiang, M. (2023). Mesencephalic astrocyte-derived neurotrophic factor (MANF) prevents the neuroinflammation induced dopaminergic neurodegeneration. *Experimental Gerontology*, *171*, 112037. https://doi.org/10.1016/j.exger.2022.112037

Zhang, X., & Zang, Z. (2023). Evaluate the efficacy and reliability of functional gradients in within-subject designs. *Human Brain Mapping*, *44*(6), 2336–2344. https://doi.org/10.1002/hbm.26213

Zhao, K., Zheng, Q., Dyrba, M., Rittman, T., Li, A., Che, T., Chen, P., Sun, Y., Kang, X., Li, Q., Liu, B., Liu, Y., & Li, S. (2022). Regional radiomics similarity networks reveal distinct subtypes and abnormality patterns in mild cognitive impairment. *Advanced Science*, *9*(12), e2104538. https://doi.org/10.1002/advs.202104538

Zhao, L., Wang, D., Xue, S. W., Tan, Z., Wang, Y., & Lian, Z. (2021). Aberrant state-related dynamic amplitude of low-frequency fluctuations of the emotion network in major depressive disorder. *Journal of Psychiatric Research*, *133*, 23–31. https://doi.org/10.1016/j.jpsychires.2020.12.003

Zhou, H. X., Chen, X., Shen, Y. Q., Li, L., Chen, N. X., Zhu, Z. C., Castellanos, F. X., & Yan, C. G. (2020). Rumination and the default mode network: Meta-analysis of brain imaging studies and implications for depression. *NeuroImage*, *206*, 116287. https://doi.org/10.1016/j.neuroimage.2019.116287

SUPPORTING INFORMATION

Additional supporting information can be found online in the Supporting Information section at the end of this article.

How to cite this article: Xiao, Y., Zhao, L., Zang, X., & Xue, S.-W. (2023). Compressed primary-to-transmodal gradient is accompanied with subcortical alterations and linked to neurotransmitters and cellular signatures in major depressive disorder. *Human Brain Mapping*, *44*(17), 5919–5935. https://doi.org/10.1002/hbm.26485